






Mechanisms of one-photon two-site double ionization after resonant inner-valence excitation in Ne clusters

Andreas Hans ^{1,*}, Florian Trinter ^{2,3}, Philipp Schmidt ^{1,4}, Sebastian Eckart,² Sven Grundmann,² Gregor Hartmann,^{1,5} Xaver Holzapfel,¹ Carolin Honisch,¹ Gregor Kastirke,² Max Kircher,² Niklas Melzer,² Christian Ozga,¹ Clemens Richter,³ Jonas Rist,² Markus Schöffler,² Daniel Trabert,² Isabel Vela-Perez,² Johannes H. Viehmann,¹ Miriam Weller,² Reinhard Dörner,² Uwe Hergenhahn ³, Arno Ehresmann,¹ André Knie ¹, Kirill Gokhberg,⁶ Aryya Ghosh,⁷ and Till Jahnke^{4,†}

¹Universität Kassel, Institut für Physik und CINSaT, Heinrich-Plett-Straße 40, 34132 Kassel, Germany

²Goethe-Universität, Institut für Kernphysik, Max-von-Laue-Straße 1, 60438 Frankfurt am Main, Germany

³Fritz-Haber-Institut der Max-Planck-Gesellschaft, Faradayweg 4-6, 14195 Berlin, Germany

⁴European XFEL, Holzkoppel 4, 22869 Schenefeld, Germany

⁵Helmholtz-Zentrum Berlin (HZB), Albert-Einstein-Straße 15, D-12489 Berlin, Germany

⁶Theoretische Chemie, Physikalisch-Chemisches Institut, Universität Heidelberg, Im Neuenheimer Feld 229, 69120 Heidelberg, Germany

⁷Department of Chemistry, Ashoka University, Rajiv Gandhi Education City, Sonapat, Haryana 131029, India



(Received 4 July 2022; accepted 22 December 2022; published 30 January 2023)

The role of interatomic and intermolecular energy and charge-transfer processes in weakly bound matter is currently lively debated due to emerging destructive low-energy electrons and radicals. Here, we discuss two mechanisms of single-photon two-site double ionization occurring competitively or subsequently to resonant interatomic Coulombic decay (rICD) in inner-valence ($2s \rightarrow np$) excited Ne dimers and clusters. The first mechanism is photoelectron-impact ionization which is, in general, not related to resonant excitation, but in the present case strongly enhanced and, thus, observable due to resonant excitation. Studying this mechanism at its energetic threshold enables addressing a subset of Ne dimers with selected bond lengths. The second mechanism is collisional ionization of energetic Rydberg atoms, which are produced by rICD in Ne clusters and may be ionized by collisions with neutrals on their way through the medium. Both mechanisms are identified by the coincident detection of charged products and, for the case of collisional ionization, confirmed by calculations. These mechanisms produce one more low-energy electron and ion than conventional rICD and, thus, should be considered in the discussion of the biochemical impact of photoinduced rICD processes.

DOI: [10.1103/PhysRevResearch.5.013055](https://doi.org/10.1103/PhysRevResearch.5.013055)

I. INTRODUCTION

Low-energy electrons (LEEs), ions, and radicals, emerging in dense matter upon the exposure to ionizing radiation are a main mediator of radiation damage [1–4] due to their ability to induce severe damage to the basic structures of living organisms, e.g., DNA molecules. Because of the complexity of the damaging mechanisms, however, the details of the radiation damage remain poorly understood on a molecular level. Among the unsolved issues is the exact number and location of emergence of genotoxic particles per single photon-molecule interaction. Furthermore, the precise quantification of contributions from direct damage, induced directly by the ionization event, and indirect damage, induced by secondary processes, is still an open question [5].

In the recent decades, theoretical and experimental progress revealed that, contrary to isolated atoms, in weakly

bound clusters a variety of interatomic (intermolecular) charge- or energy-transfer processes may occur upon photoionization or electronic excitation [6]. Many of these processes result in nonlocal autoionization or charge redistribution with important consequences for the reaction products of light-matter interactions. By now, interatomic Coulombic decay (ICD) and a plethora of related processes have been investigated in detail in many different systems, ranging from prototypical noble-gas clusters to microhydrated biomolecules and liquid water [7]. Since typically LEEs and energetic ions are the results of such processes, the relevance of interatomic decay mechanisms in real-life systems is currently lively debated.

On the one hand, the local emission of LEEs due to ICD or related processes may contribute to radiation damage in biological tissue after exposure to ionizing radiation (e.g., ultraviolet or x-ray photons) by causing single-, double-, multiple-strand breaks [1,8], or clustered damage [9]. On the other hand, this damage could be introduced on purpose using certain marker elements in radiation therapies [5,10]. To the best of our knowledge, ICD has, however, not yet been observed directly to cause radiation damage in biological systems.

Regarding radiobiological relevance, the resonant variant of ICD, resonant interatomic Coulombic decay (rICD), is

*hans@physik.uni-kassel.de

†till.jahnke@xfel.eu

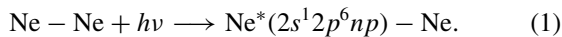
Published by the American Physical Society under the terms of the [Creative Commons Attribution 4.0 International](https://creativecommons.org/licenses/by/4.0/) license. Further distribution of this work must maintain attribution to the author(s) and the published article's title, journal citation, and DOI.

of particular interest, occurring, e.g., after resonant inner valence excitation or as part of decay cascades after resonant Auger decay [11–13]. Resonant excitation allows the element-, site-, and state-selective release of genotoxic reaction products, making it a promising candidate for targeted radiation therapies [10,14]. It is, therefore, all the more important to understand the number and properties of rICD reaction products in detail.

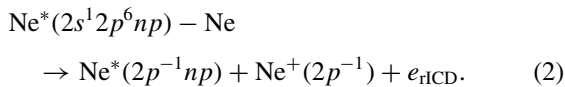
In the present paper, we focus on mechanisms resulting in emission of two LEEs from Ne dimers and clusters after absorption of a single photon. Single-photon double ionization is a well-studied process in isolated atoms [15–17] and molecules [18,19] giving access to the investigation of electron correlation. In extended systems, such as prototypical clusters, additional channels for double ionization open due to correlations between neighbors and collisions of outgoing particles.

Here, we demonstrate that rICD produces more LEEs and ions than hitherto considered. In contrast to related processes, in the present example the destructive effect is not constrained to the location of the site of photoexcitation, but further LEEs and ions emerge along the path of the primary reaction products. Additionally, we demonstrate that also rICD's main competitor, local autoionization, may produce LEEs and ions with specific properties by electron-impact ionization.

Resonant ICD was first observed in Ne clusters [11]. It can occur, for example, after $2s \rightarrow np$ resonant excitation of one Ne atom in a cluster, exemplified by a dimer in Eq. (1),



The np electron acts as a spectator during rICD, i.e., it remains in its bound orbital. rICD may be described as



Consequently, free Rydberg atoms are produced in rICD, which was confirmed by the observation of fluorescence subsequent to rICD [20]. Although the Ne Rydberg atom is neutral, the delocalization of the Rydberg electron makes the Ne^+ ion and the Ne^* core feel a net repulsive Coulomb force. Indeed, energetic Ne^+ ions were experimentally observed for rICD following $2s$ excitation to Rydberg orbitals with $n \geq 4$ [21]. The kinetic-energy release (KER) of the ion-Rydberg pair converges to the value of 2.3 eV for high n , which is observed for purely ionic $\text{Ne}^+ - \text{Ne}^+$ repulsion [22], and is somewhat lower for low n due to screening by the Rydberg electron, namely, 1.5 eV for $n = 4$ and 1.7 eV for $n = 5$. The Coulomb explosion can be assumed to be symmetric, i.e., the Rydberg atom will gain the same kinetic energy as the Ne^+ ion. As we will demonstrate below, the Rydberg atom has enough kinetic energy to be ionized in collisions with neutrals on their way through the medium.

Resonant ICD as described in Eq. (2) is not the only decay path of the resonantly excited Ne. In isolated Ne atoms, local autoionization is the dominant mode of relaxation, sketched in Eq. (3), and only for very high n fluorescence emission becomes competitive [23],

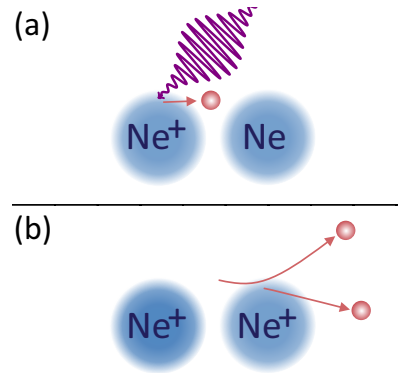
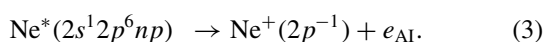
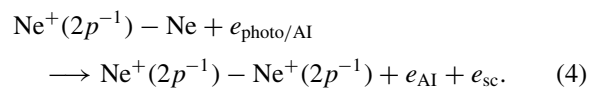


FIG. 1. Illustration of the two-step photoelectron-impact ionization in a Ne dimer. (a) An electron is released from one atom, either by direct photoionization or, e.g., by autoionization of an excited state. (b) The first electron impacts on the neighboring atom and releases a secondary electron.

In the photon-energy-dependent ionization cross section of atoms, the interference between direct $2p$ photoionization and $2s \rightarrow np$ excitation followed by autoionization is the reason for pronounced asymmetric Fano resonances [24,25]. Theoretical estimates for Ne dimers predict autoionization to dominate also over rICD for the lowest $2s \rightarrow np$ excitation, i.e., for $n = 3$ [26]. For $n = 4$ and $n = 5$, however, both processes are about equally probable with increasing probability for rICD for higher n . Although autoionization does not produce any LEEs directly, the resulting fast electron may do so by inelastic scattering in the environment. In detail, this mechanism can be regarded as a two-step process. First, a fast electron is produced by either direct photoionization or autoionization of the resonance. Second, the electron travels towards a neighboring atom and knocks off another electron in a $(e, 2e)$ collision. For the case of the Ne dimer, the second step can be written as



The process of photoelectron-impact ionization is sketched in Fig. 1. This mechanism is known to be the origin of a pronounced background of LEEs in electron-spectroscopy experiments on dense samples [27]. The properties of (photo-)electron-impact ionization are accessible in experiments on small systems and have been studied in detail for the He dimer [28].

The two electrons originating from the photoionization/autoionization ($e_{\text{photo/AI}}$) and the scattering process (e_{sc}) share a fixed amount of energy, which can be determined by

$$E_{\text{kin}, e_{\text{photo/AI}}} + E_{\text{kin}, e_{\text{sc}}} = h\nu - 2\text{IP} - \text{KER}. \quad (5)$$

Here, $h\nu$ is the exciting-photon energy and IP is the one-site single-ionization potential. The KER of the two resulting ions is a function of the internuclear distance R at the moment of the second ionization event. In the classical reflection approximation, which is valid for the Ne dimer [28], the KER of two singly charged ions can be calculated from the Coulomb

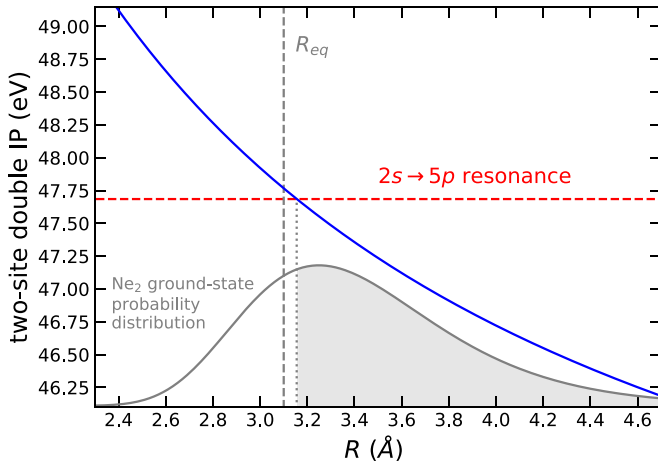


FIG. 2. Two-site DIP of the Ne dimer as a function of the internuclear distance R between the two Ne atoms (solid blue line). The energetic positions of the $2s \rightarrow 5p$ resonance (dashed red horizontal line) and the dimer ground-state equilibrium distance R_{eq} (dashed gray vertical line) are indicated. The probability distribution of R in the Ne dimer ground state is sketched on an arbitrary probability axis (taken from Ref. [28]). On the resonance, only dimers with internuclear distances larger than 3.15 \AA can be ionized (see discussion in Sec. II B), indicated by the gray shaded region to the right of the dotted gray line. In general, for a given photon energy, only the subset with R larger than the intersection point of photon energy and DIP curve can be subject to double ionization.

law as

$$\text{KER} = \frac{e}{4\pi\epsilon_0 R}, \quad (6)$$

providing the KER in convenient units of eV and using the elementary charge e and the vacuum permittivity ϵ_0 . In the present paper, we intend to study the appearance of LEEs and, therefore, investigate photoelectron-impact ionization at its energetic threshold. It is obvious that, if the exciting-photon energy only slightly exceeds the threshold energy $2 \text{ IP} + \text{KER}(R)$, both emitted electrons are slow. The two-site double ionization potential (DIP) as a function of the internuclear distance R is shown in Fig. 2, calculated according to Eq. (6) plus twice the asymptotic atomic IP (21.56 eV).

Close to the energetic threshold, photoelectron-impact ionization is elusive due to the low cross section. In the example of Ne dimers, however, we take advantage of the fact that the $2s \rightarrow 5p$ resonance is located just at the threshold energy of electron-impact ionization (dashed red line in Fig. 2). The resonant excitation and subsequent production of photoelectrons by autoionization considerably enhances the probability for photoelectron-impact ionization and makes it observable. As we will see below, fine-tuning of the exciting-photon energy allows for selective production of ion pairs at defined internuclear distances.

In Sec. II, we will first discuss the two-site double ionization of the Ne dimer by electron-impact ionization in the vicinity of the $2s \rightarrow 5p$ resonance. In Sec. III, we describe the collisional ionization of Rydberg atoms formed by rICD in larger Ne clusters.

II. BOND-LENGTH-SELECTIVE PHOTOELECTRON-IMPACT IONIZATION IN NE DIMERS

A. Experiment

The experiments were carried out at the XUV beamline UE112_PGM-1 of the synchrotron BESSY II (Helmholtz-Zentrum Berlin, Germany) [29] in the single-bunch timing mode (bunch spacing 800 ns), using linear horizontally polarized photons of 47.62–47.71 eV photon energy generated by its elliptical undulator, repeatedly scanning the photon energy across the maximum of the gas-phase Ne $2s \rightarrow 5p$ resonance at 47.69 eV [21,30]. We used a mobile cold target recoil ion momentum spectroscopy (COLTRIMS) reaction microscope [31–33] for our studies, see also Ref. [34]. The Ne dimers were provided in a supersonic gas jet, which passed through two skimmers (300- μm diameter each) and was crossed with the photon beam at a right angle. We used a gas mixture of 70% Ne and 30% He, a driving pressure of 6.3 bars, and a gas nozzle of 5- μm diameter cooled down to 85 K, and achieved a few percent of Ne dimers in our supersonic gas jet whereas larger clusters were still absent. The employed COLTRIMS spectrometer consisted of an ion arm of 7-cm acceleration length and an electron arm of 6-cm acceleration and 12-cm drift length (Wiley-McLaren time-of-flight focusing geometry). Both were equipped with a microchannel plate detector (active area of 120-mm diameter) with hexagonal delay-line position readout [35,36]. Electrons and ions were guided by homogeneous electric (3.6-V/cm) and magnetic (2.55-G) fields onto the two time- and position-sensitive detectors. The field strengths were selected such that 4π sr collection solid angle for electrons and ions has been achieved for electrons up to 6-eV kinetic energy and molecular fragmentation in Ne^+/Ne^+ pairs with a KER up to 8 eV. From the times of flight and the positions of impact, the three-dimensional momentum vectors of all charged fragments of the photoreaction were retrieved as well as all derived quantities, e.g., kinetic energies and emission angles. The ionic fragments were detected in coincidence with two low-energy electrons. The coincident detection of the ionic fragments provides further information: The orientation of the dimer in the laboratory frame can be deduced. This is possible if the breakup of the dimer happens rapidly after the decay, and, accordingly, the dimer does not have time to rotate [37,38]. Therefore, also the angle between molecular axis and polarization vector is one of our possible observables.

B. Results and discussion

The process of photoelectron-impact ionization [($e, 2e$) knock off] has been well studied in the He dimer [28]. As discussed in Sec. I, the cross section of this mechanism is expected to be enhanced on the Ne dimer $2s \rightarrow 5p$ resonance due to autoionization [Eq. (3)]. The yield of quadruple coincidences of two LEEs and two Ne^+ ions as a function of the exciting-photon energy across the $2s \rightarrow 5p$ resonance is shown in Fig. 3, and the resonance structure is clearly visible.

We observe the center of the resonance at 47.685 eV. The resonance energy should be different for Σ and Π resonance states, and, therefore, depend on the angle θ between the dimer axis and the polarization vector of the exciting radiation

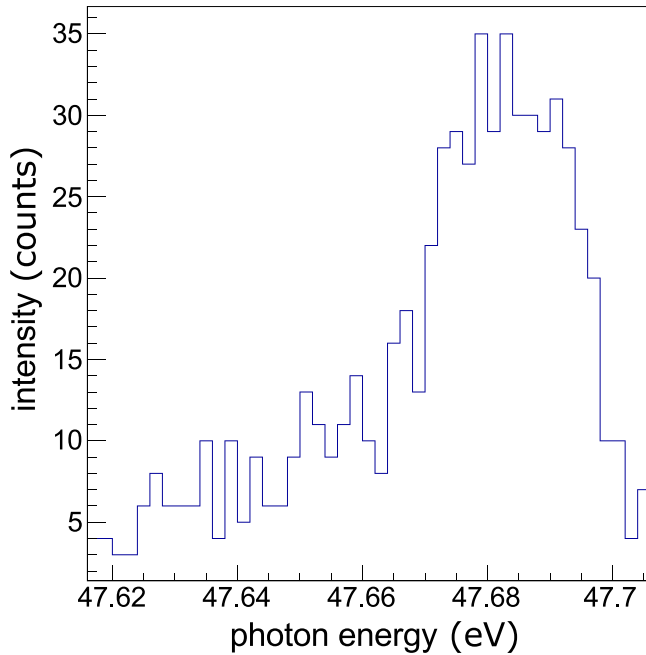


FIG. 3. Yield of Ne^+/Ne^+ ion pairs in coincidence with two low-energy electrons across the $2s \rightarrow 5p$ resonance in Ne dimers.

as has been observed and discussed before [21]. We confirm this by plotting the coincidence counts as a function of the exciting-photon energy and $\cos(\theta)$ in Fig. 4 and observe about 47.68 eV for Π and about 47.69 eV for Σ excitations. These values are shifted slightly to lower energies compared to the atomic reference value of 47.693 eV [39]. Due to the low statistics of the quadruple coincidences, these values seem to be less accurate than those of Ref. [21], which reported

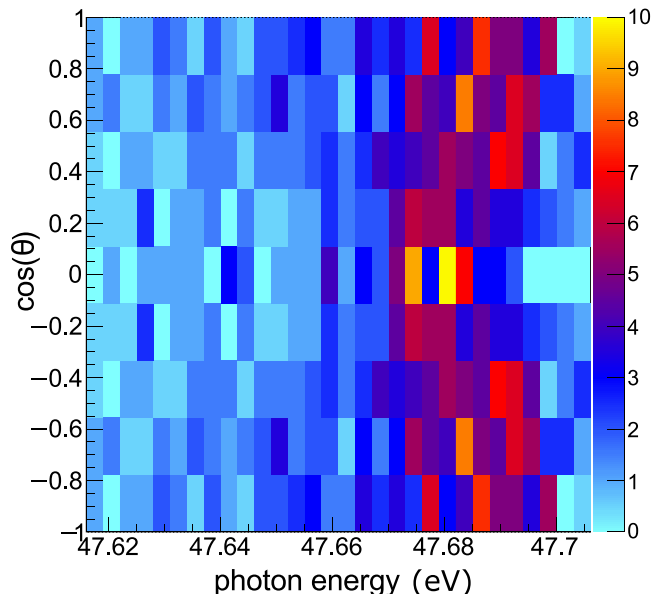


FIG. 4. Fourfold coincidence counts as functions of both the exciting-photon energy and the cosine of the angle between the Ne dimer molecular axis and the polarization vector of the incoming light. Σ and Π excitations show different excitation energies.

somewhat larger shifts of -30 meV for Π and -13 meV for Σ states.

Fortunately, the energetic threshold for knock-off ionization at the Ne dimer ground-state equilibrium distance is very close to the $2s \rightarrow 5p$ resonance. According to Fig. 2, the two-site DIP at the Ne_2 equilibrium distance (3.1 Å), indicated by the dashed vertical line, is 47.76 eV. The minimum distance at which two Ne atoms can be ionized with the photon energy at the center of the $2s \rightarrow 5p$ resonance 47.685 eV is 3.15 Å (dotted vertical line in Fig. 2), with zero kinetic energy left for the electrons. This means, if the exciting-photon energy is tuned to the $2s \rightarrow 5p$ resonance, only the dimers with a bond length larger than 3.15 Å at the moment of photoionization can be two-site doubly ionized. These dimers correspond to the gray shaded area in the Ne_2 ground-state probability distribution in Fig. 2, which has been taken from Ref. [28].

The vicinity of a resonance is no principle prerequisite for fine-tuning of the exciting-photon energy to address a subset of dimers of a certain bond length. The cross section of electron-impact ionization is, however, low when the excess energy is very low, and the enhanced production of photoelectrons on the resonance is a convenient advantage to study this phenomenon in the Ne dimer. Tuning the exciting-photon energy, e.g., to the $2s \rightarrow 4p$ resonance at about 47.10 eV [21] would select an even smaller subset of dimers with bond lengths longer than 3.6 Å.

We envision the observed effect to be applied for steering the fragmentation of larger molecules. In an extended system, the range of tunable energies is much larger than in the present prototype example. By tuning the exciting-photon energy precisely, two electronic vacancies may be created at defined sites by the knock-off mechanism which results in dissociation.

III. COLLISIONAL IONIZATION OF ENERGETIC RYDBERG ATOMS FORMED BY RESONANT ICD IN NE CLUSTERS

A. Experiment

In a second experiment we investigated in more detail the emission of LEEs in the context of rICD following $2s \rightarrow 4p$ and $2s \rightarrow 5p$ excitations in larger Ne clusters. Also this second experiment was performed at the UE112_PGM-1 beamline of BESSY II, see Sec. II A. The setup has been described in detail in several previous publications [40–42]. Briefly, it consists of two chambers, separated by a 1-mm skimmer. The cluster jet is produced by supersonic expansion of Ne gas through a conical copper nozzle of a 30° opening angle and $80\text{-}\mu\text{m}$ diameter. The nozzle is cryogenically cooled by a constant flow of liquid He. The measurements were conducted at 50 K and 1.2 bars driving pressure. Using empirical scaling laws, the mean cluster size of the resulting jet can be estimated to be $\langle N \rangle = 270$ [43].

In the main chamber, the cluster jet was crossed with linearly polarized monochromatic synchrotron radiation. At exciting-photon energies around the Ne $2s$ edge, the photon bandwidth was about 6 meV. Electrons emitted at the crossing point of cluster jet and synchrotron radiation were detected by a magnetic bottle time-of-flight electron spectrometer. The time of flight of each electron was determined by measuring

each individual detector event with respect to a reference clock synchronized to the circulation of the electron bunch in the storage ring, which was operated in the single-bunch mode, i.e., providing an exciting-photon pulse every 800 ns. The time-of-flight axis was calibrated to electron kinetic energies using well-known photoemission lines of Ne atoms. Since electron coincidences are measured as two events on the same detector, dead times of the electronics result in a narrow blind window of kinetic energies in which no coincidences can be detected. A common procedure using data acquisition during the time interval of two consecutive excitation pulses was used to eliminate random coincidences in the electron spectra [44].

B. Theory

As a complement to the experimental study on the kinetic energies of the electrons and ions produced by rICD, we calculated the potential-energy curves (PECs) of the rICD final states, i.e., $\text{Ne}^*(2p^{-1}np)\text{-Ne}^+(2p^{-1})$ states, to identify their character (bound or dissociative) and to estimate the KER of possible dissociation products.

The computation of accurate $\text{Ne}^*(2p^{-1}np)\text{-Ne}^+(2p^{-1})$ PECs is very challenging due to their Rydberg character. Their accurate description requires high-level *ab initio* methods as well as carefully chosen basis sets. We computed the PECs using the equation-of-motion coupled cluster singles and doubles method as implemented in the GAMES-US software packages. In our calculations, we used restricted open-shell Hartree-Fock reference states. For the computation of PECs of $\text{Ne}^*(2p^{-1}np)\text{-Ne}^+(2p^{-1})$ states, we started initially from positively charged ionized states and finally computed the excited states.

To find an appropriate basis set, we started from the cc-pVTZ basis set and externally added $7p$ functions on both Ne atoms in an evenly tempered manner. The external p functions have been generated with a ratio of 2.5 starting from the lowest coefficient of the p -type function of the cc-pVTZ basis set. In our calculations, D_{2h} symmetry has been used. We computed the PECs in the six irreducible representations. In the B_{2u} irreducible representation, we have computed the PECs for the seven lowest $\text{Ne}^*(2p^{-1}np)\text{-Ne}^+(2p^{-1})$ states. Among the seven states, five states are dissociative and two states are bound ones. From the PECs of dissociative character, we estimated the amount of KER of each dissociation product. To estimate the KER of individual Ne atoms from the PEC, we first considered the energy at the ground-state equilibrium geometry of Ne_2 , and later on we considered the energy at a very large distance between two Ne atoms. Finally, we computed the energy difference between these two geometries. From the computed PECs in the B_{2u} representation, we estimated that each Ne atom can gain kinetic energy between 1.4 and 1.85 eV. Figure 5 represents the PECs in the B_{2u} irreducible representation.

Analogously, we have also computed the PECs for the eight lowest $\text{Ne}^*(2p^{-1}np)\text{-Ne}^+(2p^{-1})$ states in B_{2g} , the five lowest states in B_{1g} , and the nine lowest states in B_{1u} , the six lowest states in A_g , and the nine lowest states in A_u irreducible representations. All of them show similar behavior, namely, that most of the states are repulsive and the resulting

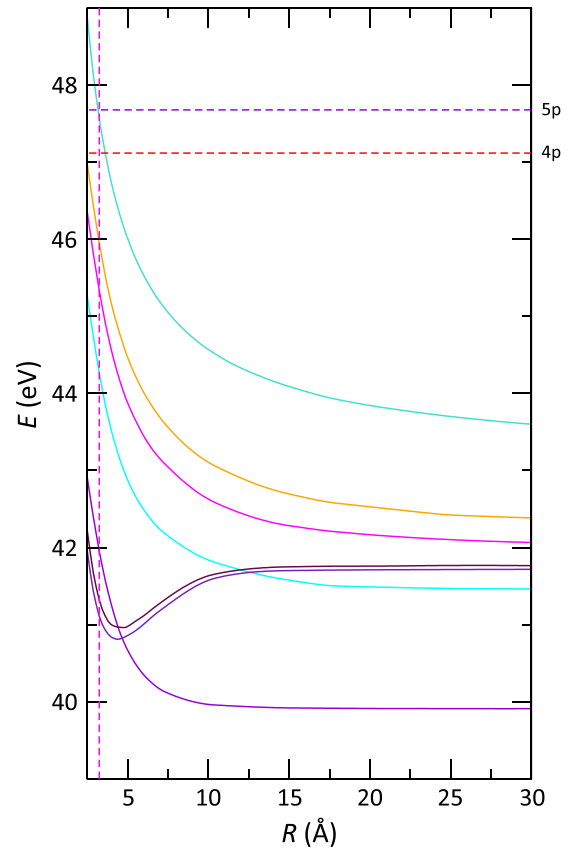


FIG. 5. PECs of the seven lowest $\text{Ne}^*(2p^{-1}np)\text{-Ne}^+(2p^{-1})$ states in the B_{2u} irreducible representation. The dashed vertical line indicates the equilibrium distance in the neutral Ne dimer.

fragments obtain kinetic energy in the range of about 1.4–2.0 eV.

C. Results and discussion

The main experimental result of this study is presented in Fig. 6. It shows the KER of two Ne^+ ions for different exciting-photon energies on and off the $2s \rightarrow np$ resonances for $n = 4, 5$, now measured for larger clusters. Due to the constraints of the experiment, we would not measure a fourfold coincidence of two ions and two electrons, but we infer the creation of two Ne^+ ions in a single-ionization event from the coincident detection of two LEEs. The KER is not measured directly in this experiment. However, since asymptotically all Coulomb repulsion will be converted to KER, it can be calculated as difference of the energy available through resonant excitation $h\nu_{\text{exc}}$ and the sum of the kinetic energies of two LEEs, $E_{\text{kin}1}$ and $E_{\text{kin}2}$, detected in coincidence, and two times the ionization potential $\text{IP}_{\text{cluster}}$ of Ne atoms bound in a cluster,

$$\text{KER} = h\nu_{\text{exc}} - E_{\text{kin}1} - E_{\text{kin}2} - 2\text{IP}_{\text{cluster}}. \quad (7)$$

$\text{IP}_{\text{cluster}} = 20.9$ eV is determined under the same experimental conditions via $\text{IP}_{\text{cluster}} = h\nu_{\text{exc}} - E_{\text{kin},2p}$ by measuring the $2p$ photoelectron kinetic energy $E_{\text{kin},2p}$. It is shifted to lower binding energies compared to the atomic value due to final-state polarization. Only coincidence events of two LEEs with kinetic energies below 10 eV are considered in the

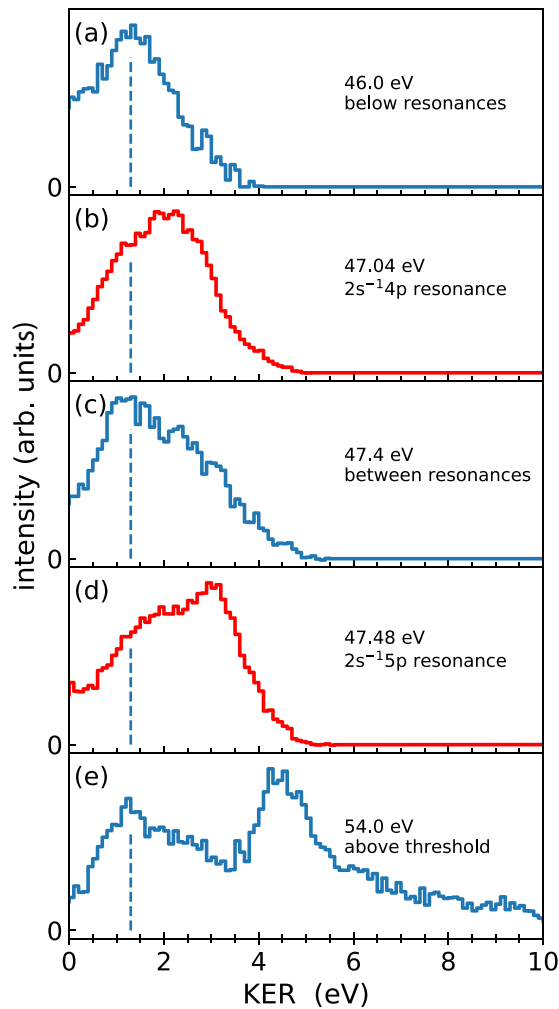


FIG. 6. KER of two resulting Ne^+ ions for different exciting-photon energies on and off resonance, experimentally determined by applying Eq. (7). (a) Below the $2s \rightarrow 4p$ resonance. (b) On the $2s \rightarrow 4p$ resonance. (c) Between the $2s \rightarrow 4p$ and $2s \rightarrow 5p$ resonances. (d) On the $2s \rightarrow 5p$ resonance. (e) Above the $2s$ ionization threshold. For better visualization, the two spectra measured on resonance are shown in red.

analysis. For all spectra, the exciting-photon energy is well below the one-site Ne^{2+} double-ionization potential, which is at about 62.5 eV [45]. The two LEEs, hence, must be emitted from two different Ne atoms within the cluster.

The blue spectra in Figs. 6(a) and 6(c) have been taken off-resonance and below the Ne $2s$ ionization potential. There is a single feature observed, peaking at a KER of 1.3 eV (indicated by the vertical dashed lines in all panels). The peak in the KER spectrum corresponds to Coulomb repulsion of two ions at the internuclear distance of 11.1 Å. There is no electron correlation which is able to act over this distance. The only possible way to create two LEEs at distant sites is via photoelectron-impact ionization, just as in Sec. II and illustrated in Fig. 7 (see also Ref. [42]). Contrary to the dimer case, however, in clusters the $(e, 2e)$ collision can take place at much larger distances and, therefore, at lower onset energies. The KER peak at 1.3 eV represents the most likely distance of the collision. The impact-ionization cross section depends on the electron's

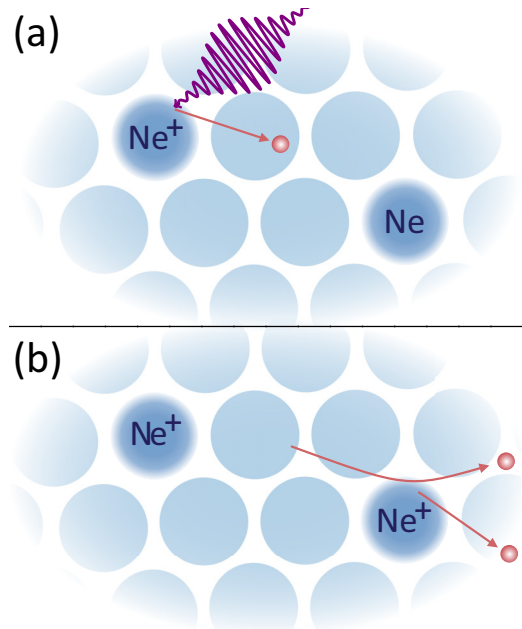


FIG. 7. Illustration of the electron-impact ionization in a large Ne cluster. (a) An electron is released from one atom in the cluster either by direct photoionization (as shown) or, e.g., by autoionization. (b) On its way through the cluster, the electron impacts on another Ne atom and releases a secondary electron. Compared to the dimer case (see Fig. 1), this process can happen at much larger distances, i.e., the first electron may pass several atoms and impact on a remote other Ne atom. The distance between the two sites is reflected in the KER of the ions and the kinetic energy of the resulting electrons.

kinetic energy, which explains small deviations of the shape of this feature in the spectra. The spectrum in Fig. 6(a) has been taken at 46.0 eV, i.e., $46.0 \text{ eV} - 2 \cdot 20.9 \text{ eV} = 4.2 \text{ eV}$ are left for the kinetic energy of the ions and the shortest possible distance for electron-impact ionization is 3.4 Å. Given the fact that two electrons with close to zero kinetic energies cannot be detected in coincidence (see Sec. III A) and that cross sections for impact ionization are low at these low excess energies, the experimentally observed onset at 4.0 eV in Fig. 6(a) is in good agreement. In line with these considerations, the onset shifts to about 5.4 eV in the spectrum in Fig. 6(c), taken at 47.4 eV and, thus, at 1.4-eV higher photon energy than the spectrum in Fig. 6(a). Therefore, at 47.4 eV, Ne atoms as close as 2.6 Å can be ionized by photoelectron impact.

Above the $2s$ ionization potential, a second feature appears in the spectrum [Fig. 6(e)], peaking at KER = 4.6 eV. This feature can be attributed to ICD, which is very fast and happens close to the Ne_2 equilibrium distance of 3.1 Å [22]. Importantly, from this feature we confirm that our method of KER determination from the kinetic energy of the two emitted electrons is valid. The spectra in Figs. 6(b) and 6(d) have been measured on the $2s \rightarrow 4p$ and $2s \rightarrow 5p$ resonances, respectively. Pure rICD cannot contribute to these spectra since it only produces a single LEE. The experimental results show, however, that there is another process at play which produces a second LEE. Although it cannot fully be disentangled from the contribution of electron-impact ionization, the KER of this additional process corresponds to distances intermediate be-

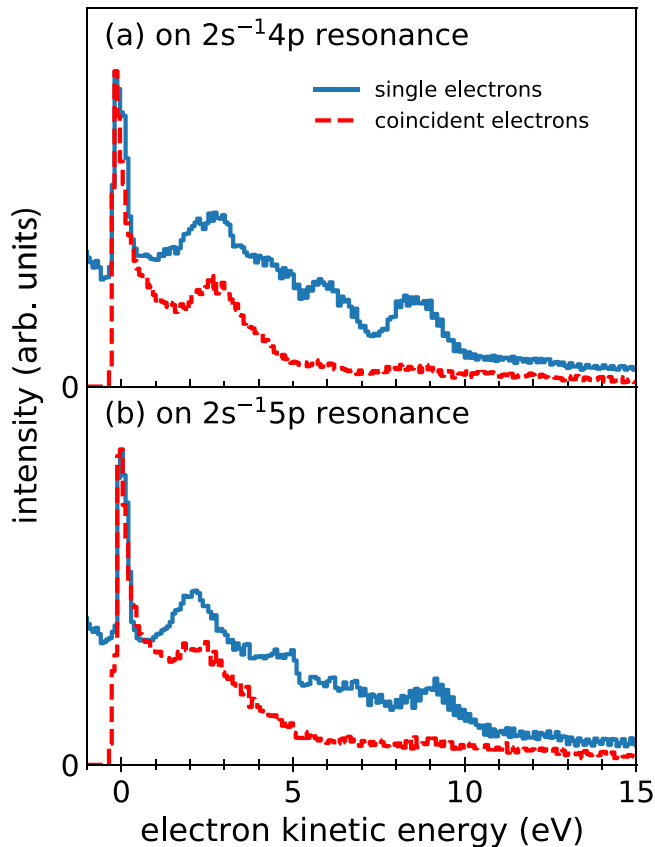


FIG. 8. Spectra of single low-energy electrons (blue traces) and coincident pairs (each electron counted individually) of two low-energy electrons (red traces) on (a) the $2s \rightarrow 4p$ resonance and (b) the $2s \rightarrow 5p$ resonance.

tween the equilibrium Ne_2 distance and the average distance of electron-impact ionization.

To elucidate the nature of the underlying process leading to emission of the second LEE, we compare the spectra of singly and pairwise emitted LEEs on the resonances in Fig. 8. The features observed in the single LEE spectra (blue curves) are well known [11]. Most prominent are the features caused by rICD peaking at about 2.5 eV for the $2s \rightarrow 4p$ resonance and about 2.0 eV for the $2s \rightarrow 5p$ resonance. Shape and energetic positions of these features agree well with the spectra of rICD electrons observed in earlier work [11]. Note that the assignment of the $2s \rightarrow np$ resonance series has been refined after the first work on rICD in Ne clusters [46]. Features at higher kinetic energies can be attributed to excitons excited by photoelectron impact [11,47,48]. In this mechanism, the emitted photoelectron loses a predefined amount of energy by scattering at a neutral atom, exciting it into an excitonic state. The energetic position of the main feature originating from exciton excitation can be estimated by subtracting the binding energy of the photoelectron (about 21 eV for Ne clusters) and the lowest excitonic excitation in Ne (between 17 and 18 eV) from the photon energy (47.04 eV on the $2s \rightarrow 4p$ resonance) [47]. The residual kinetic energy of the scattered electron is, thus, between 8 and 9 eV and matches well with the observation in Fig. 8(a). Further features from excitation of higher excitonic states appear at lower kinetic energies.

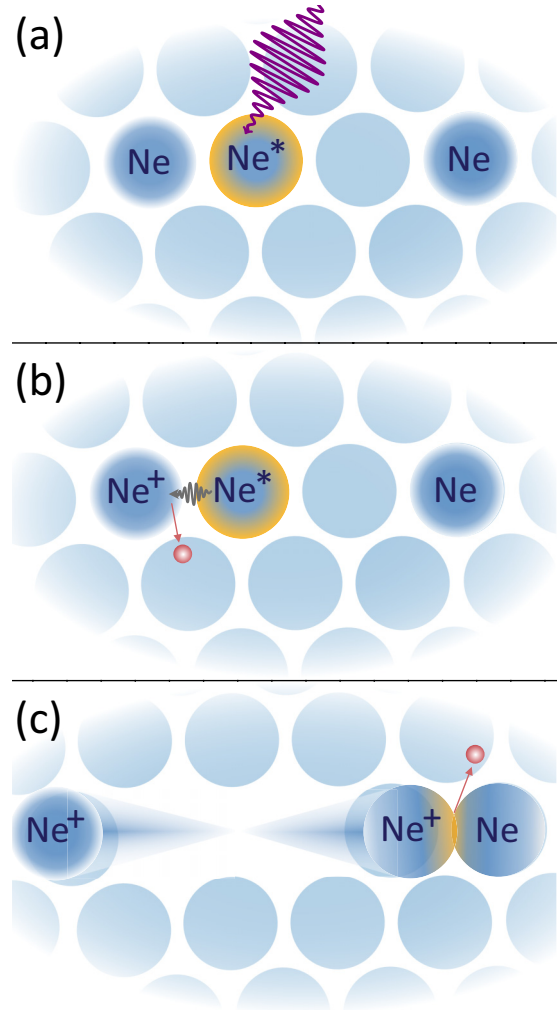


FIG. 9. Illustration of the collisional ionization observed in the cluster. (a) Resonant photoexcitation of one atom in the cluster. (b) Resonant interatomic Coulombic decay with emission of a slow electron. (c) Coulomb explosion and subsequent collision of the Rydberg atom with a neutral partner, releasing the Rydberg electron by using part of the kinetic energy of the Ne^* atom.

Additionally, a feature peaking at zero kinetic energy is observed. Electron-impact ionization and multiple-scattering processes contribute to this common phenomenon in spectra of dense samples [27]. Note that the spectrometer used in the pioneering work on rICD [11] was much less sensitive to zero-kinetic-energy electrons compared to the magnetic bottle spectrometer used in the present experiment.

Let us now discuss possible mechanisms explaining the emission of two LEEs after resonant excitation, resulting in higher KER of the ions and, thus, happening at shorter distances than electron-impact ionization. From the decay of electronic excitations in atoms, it is well known that two electrons can be emitted simultaneously due to electron correlation, consider, e.g., double Auger decay [49–52]. In clusters, recently a variant of ICD was observed which emits two LEEs due to interatomic energy transfer [53,54]. We can rule out such correlative mechanisms in the present case for mainly two reasons. First, these processes can be considered to happen instantaneously compared to nuclear motion, implying

that both electrons would be emitted simultaneously at the Ne₂ equilibrium distance. From the KER spectra on resonance in Fig. 6, however, we see that the two electrons are created further apart. Second, in correlative effects the electrons share their energy. From comparison of the spectra of single LEEs (blue curves) with those of pairwise emitted LEEs (red curves) in Fig. 8, it becomes clear that this is not the case, but that one of the detected electrons has the same kinetic energy as the electrons emitted due to rICD. These facts suggest that the two electrons are emitted in a cascade of two steps, the first of which is rICD. The resulting neutral Rydberg atoms, produced in an Ne* $2p^{-1}nl$ configuration, cannot autoionize as their internal energy does not exceed the ionization potential.

The only possible mechanism for the second ionization seems to be the collision of the Rydberg atoms with other neutral atoms. Since the orbit radius of the $4p/5p$ electron exceeds the Ne₂ internuclear distance, it can be assumed that in the Coulomb explosion the Ne Rydberg atom and the Ne⁺ ion separate symmetrically with identical amounts of kinetic energy. The values observed experimentally for energetic ions on the $2s \rightarrow 4p$ and $2s \rightarrow 5p$ resonances are 1.5 and 1.7 eV, respectively, [21]. These values are in good agreement with our theoretical estimations from the Ne*($2p^{-1}np$)-Ne+($2p^{-1}$) PECs and exceed the ionization potentials of the $2p^{-1}4p$ and $2p^{-1}5p$ Rydberg atoms, which are 1.3 and 0.8 eV, respectively, confirming that collisional ionization is possible. The three-step process of collisional ionization is sketched in Fig. 9.

IV. CONCLUSIONS

In two different coincidence experiments, we observed mechanisms of single-photon two-site double ionization after resonant $2s \rightarrow np$ photoexcitation of Ne dimers and

clusters. In the experiment on dimers, we found ($e, 2e$) photoelectron-impact ionization to be resonantly enhanced by autoionization. In the vicinity of the Ne $2s \rightarrow 5p$ resonance because of the bond-length dependence of the KER only a subset of dimers, those with bonds longer than the equilibrium distance, are accessible to double ionization.

In larger Ne clusters, energetic Rydberg atoms are produced via resonant interatomic Coulombic decay. Single and coincident electron spectra and KER spectra reveal the emission of two low-energy electrons in a cascade of two different steps, the first one being rICD and the second collisional ionization of the Rydberg atom. This interpretation is in line with earlier experimental observations of single energetic ions and our own theoretical calculations of the Ne*($2p^{-1}np$)-Ne+($2p^{-1}$) PECs.

Although resonant ICD in the radiation-damage context has so far only been discussed regarding the local emission of the ICD electron itself, our results demonstrate that, after resonant excitation of weakly bound systems, destructive low-energy electrons and ions are not only produced locally in the primary reaction. On their way through the medium, energetic reaction products emitted in competition or subsequently to the ICD electron can produce further LEEs. We believe our findings to be relevant for modeling the role of rICD in radiation damage or radiation therapy.

ACKNOWLEDGMENTS

We thank Helmholtz-Zentrum Berlin (HZB) for beamtime allocation and the BESSY II staff for assistance. The work was supported by the Federal Ministry of Education and Research of Germany (BMBF) in the framework of Project No. 05K19RK2 (GPHASE). We acknowledge P. Demekhin for fruitful discussions.

-
- [1] G. García Gómez-Tejedor and M. C. Fuss, *Radiation Damage in Biomolecular Systems* (Springer, Dordrecht, 2012).
 - [2] B. Boudaïffa, P. Cloutier, D. Hunting, M. A. Huels, and L. Sanche, Resonant formation of DNA strand breaks by low-energy (3 to 20 eV) electrons, *Science* **287**, 1658 (2000).
 - [3] E. Alizadeh and L. Sanche, Precursors of solvated electrons in radiobiological physics and chemistry, *Chem. Rev.* **112**, 5578 (2012).
 - [4] Y. Park, Z. Li, P. Cloutier, L. Sanche, and J. R. Wagner, DNA damage induced by low-energy electrons: Conversion of thymine to 5,6-dihydrothymine in the oligonucleotide trimer TpTpT, *Radiat. Res.* **175**, 240 (2010).
 - [5] E. Alizadeh, T. M. Orlando, and L. Sanche, Biomolecular damage induced by ionizing radiation: The direct and indirect effects of low-energy electrons on DNA, *Annu. Rev. Phys. Chem.* **66**, 379 (2015).
 - [6] L. S. Cederbaum, J. Zobeley, and F. Tarantelli, Giant Intermolecular Decay and Fragmentation of Clusters, *Phys. Rev. Lett.* **79**, 4778 (1997).
 - [7] T. Jahnke, U. Hergenbahn, B. Winter, R. Dörner, U. Fröhling, P. V. Demekhin, K. Gokhberg, L. S. Cederbaum, A. Ehresmann, A. Knie, and A. Dreuw, Interatomic and intermolecular coulombic decay, *Chem. Rev.* **120**, 11295 (2020).
 - [8] M. A. Huels, B. Boudaïffa, P. Cloutier, D. Hunting, and L. Sanche, Single, double, and multiple double strand breaks induced in DNA by 3-100 eV electrons, *J. Am. Chem. Soc.* **125**, 4467 (2003).
 - [9] B. M. Sutherland, P. V. Bennett, O. Sidorkina, and J. Laval, Clustered DNA damages induced in isolated DNA and in human cells by low doses of ionizing radiation, *Proc. Natl. Acad. Sci. USA* **97**, 103 (2000).
 - [10] K. Gokhberg, P. Kolorenč, A. I. Kuleff, and L. S. Cederbaum, Site- and energy-selective slow-electron production through intermolecular Coulombic decay, *Nature (London)* **505**, 661 (2014).
 - [11] S. Barth, S. Joshi, S. Marburger, V. Ulrich, A. Lindblad, G. Öhrwall, O. Björneholm, and U. Hergenbahn, Observation of resonant interatomic coulombic decay in Ne clusters, *J. Chem. Phys.* **122**, 241102 (2005).
 - [12] P. O'Keeffe, E. Ripani, P. Bolognesi, M. Coreno, M. Devetta, C. Callegari, M. Di Fraia, K. C. Prince, R. Richter, M. Alagia, A. Kivimäki, and L. Avaldi, The role of the partner atom and resonant excitation energy in interatomic coulombic decay in rare gas dimers, *J. Phys. Chem. Lett.* **4**, 1797 (2013).
 - [13] M. Kimura, H. Fukuzawa, T. Tachibana, Y. Ito, S. Mondal, M. Okunishi, M. Schöffler, J. Williams, Y. Jiang, Y. Tamenori, N. Saito, and K. Ueda, Controlling low-energy electron emis-

- sion via resonant-auger-induced interatomic coulombic decay, *J. Phys. Chem. Lett.* **4**, 1838 (2013).
- [14] F. Trinter, M. S. Schöffler, H.-K. Kim, F. P. Sturm, K. Cole, N. Neumann, A. Vredenburg, J. Williams, I. Bocharova, R. Guillemin, M. Simon, A. Belkacem, A. L. Landers, T. Weber, H. Schmidt-Böcking, R. Dörner, and T. Jahnke, Resonant Auger decay driving intermolecular Coulombic decay in molecular dimers, *Nature (London)* **505**, 664 (2014).
- [15] J. H. D. Eland, O. Vieuxmaire, T. Kinugawa, P. Lablanquie, R. I. Hall, and F. Penent, Complete Two-Electron Spectra in Double Photoionization: The Rare Gases Ar, Kr, and Xe, *Phys. Rev. Lett.* **90**, 053003 (2003).
- [16] Y. Hikosaka, P. Lablanquie, F. Penent, T. Kaneyasu, E. Shigemasa, J. H. D. Eland, T. Aoto, and K. Ito, Double Photoionization into Double Core-Hole States in Xe, *Phys. Rev. Lett.* **98**, 183002 (2007).
- [17] E. P. Månsson, D. Guénot, C. L. Arnold, D. Kroon, S. Kasper, J. M. Dahlström, E. Lindroth, A. S. Kheifets, A. L'Huillier, S. L. Sorensen, and M. Gisselbrecht, Double ionization probed on the attosecond timescale, *Nat. Phys.* **10**, 207 (2014).
- [18] P. Lablanquie, T. P. Grozdanov, M. Žitnik, S. Carniato, P. Selles, L. Andric, J. Palaudoux, F. Penent, H. Iwayama, E. Shigemasa, Y. Hikosaka, K. Soejima, M. Nakano, I. H. Suzuki, and K. Ito, Evidence of Single-Photon Two-Site Core Double Ionization of C₂H₂ Molecules, *Phys. Rev. Lett.* **107**, 193004 (2011).
- [19] J. H. D. Eland and R. Feifel, *Double Photoionisation Spectra of Molecules* (Oxford University Press, Oxford, 2018).
- [20] A. Knie, A. Hans, M. Förstel, U. Hergenhahn, P. Schmidt, P. Reiß, C. Ozga, B. Kambs, F. Trinter, J. Voigtsberger, D. Metz, T. Jahnke, R. Dörner, A. I. Kuleff, L. S. Cederbaum, P. V. Demekhin, and A. Ehresmann, Detecting ultrafast interatomic electronic processes in media by fluorescence, *New J. Phys.* **16**, 102002 (2014).
- [21] T. Aoto, K. Ito, Y. Hikosaka, E. Shigemasa, F. Penent, and P. Lablanquie, Properties of Resonant Interatomic Coulombic Decay in Ne Dimers, *Phys. Rev. Lett.* **97**, 243401 (2006).
- [22] T. Jahnke, A. Czasch, M. S. Schöffler, S. Schössler, A. Knapp, M. Käsz, J. Titze, C. Wimmer, K. Kreidi, R. E. Grisenti, A. Staudte, O. Jagutzki, U. Hergenhahn, H. Schmidt-Böcking, and R. Dörner, Experimental Observation of Interatomic Coulombic Decay in Neon Dimers, *Phys. Rev. Lett.* **93**, 163401 (2004).
- [23] P. Lablanquie, F. Penent, R. I. Hall, J. H. D. Eland, P. Bolognesi, D. Cooper, G. C. King, L. Avaldi, R. Camilloni, S. Stranges, M. Coreno, K. C. Prince, A. Mühleisen, and M. Žitnik, Observation and Characterization of the Fluorescence Decay of the 2s2p⁶np ¹P⁰ Excited States of Ne, *Phys. Rev. Lett.* **84**, 431 (2000).
- [24] K. Codling, R. P. Madden, and D. L. Ederer, Resonances in the photo-ionization continuum of Ne I (20-150 eV), *Phys. Rev.* **155**, 26 (1967).
- [25] K. Schulz, M. Domke, R. Püttner, A. Gutiérrez, G. Kaindl, G. Miecznik, and C. H. Greene, High-resolution experimental and theoretical study of singly and doubly excited resonances in ground-state photoionization of neon, *Phys. Rev. A* **54**, 3095 (1996).
- [26] S. Kopelke, K. Gokhberg, L. S. Cederbaum, and V. Averbukh, Calculation of resonant interatomic Coulombic decay widths of inner-valence-excited states delocalized due to inversion symmetry, *J. Chem. Phys.* **130**, 144103 (2009).
- [27] S. Malerz, F. Trinter, U. Hergenhahn, A. Ghrist, H. Ali, C. Nicolas, C.-M. Saak, C. Richter, S. Hartweg, L. Nahon, C. Lee, C. Goy, D. M. Neumark, G. Meijer, I. Wilkinson, B. Winter, and S. Thürmer, Low-energy constraints on photoelectron spectra measured from liquid water and aqueous solutions, *Phys. Chem. Chem. Phys.* **23**, 8246 (2021).
- [28] T. Havermeier, T. Jahnke, K. Kreidi, R. Wallauer, S. Voss, M. Schöffler, S. Schössler, L. Foucar, N. Neumann, J. Titze, H. Sann, M. Kühnel, J. Voigtsberger, A. Malakzadeh, N. Sisourat, W. Schöllkopf, H. Schmidt-Böcking, R. E. Grisenti, and R. Dörner, Single Photon Double Ionization of the Helium Dimer, *Phys. Rev. Lett.* **104**, 153401 (2010).
- [29] G. Schiwietz, M. Beye, and T. Kachel, UE112_PGM-1: An open-port low-energy beamline at the BESSY II undulator UE112, *J. Large-Scale Res. Facilities* **1**, A33 (2015).
- [30] A. Kramida, Y. Ralchenko, and J. Reader, NIST Atomic Spectra Database (ver. 5.8), [Online], <https://physics.nist.gov/asd> [2021, October 29], National Institute of Standards and Technology, Gaithersburg, MD, USA.
- [31] R. Dörner, V. Mergel, O. Jagutzki, L. Spielberger, J. Ullrich, R. Moshhammer, and H. Schmidt-Böcking, Cold Target Recoil Ion Momentum Spectroscopy: a 'momentum microscope' to view atomic collision dynamics, *Phys. Rep.* **330**, 95 (2000).
- [32] J. Ullrich, R. Moshhammer, A. Dorn, R. Dörner, L. Ph H. Schmidt, and H. Schmidt-Böcking, Recoil-ion and electron momentum spectroscopy: reaction-microscopes, *Rep. Prog. Phys.* **66**, 1463 (2003).
- [33] T. Jahnke, Th. Weber, T. Osipov, A. L. Landers, O. Jagutzki, L. Ph. H. Schmidt, C. L. Cocke, M. H. Prior, H. Schmidt-Böcking, and R. Dörner, Multicoincidence studies of photo and Auger electrons from fixed-in-space molecules using the COLTRIMS technique, *J. Electron Spectrosc. Relat. Phenom.* **141**, 229 (2004).
- [34] A. Mhamdi, J. Rist, D. Aslitürk, M. Weller, N. Melzer, D. Trabert, M. Kircher, I. Vela-Pérez, J. Siebert, S. Eckart, S. Grundmann, G. Kastirke, M. Waitz, A. Khan, M. S. Schöffler, F. Trinter, R. Dörner, T. Jahnke, and Ph V. Demekhin, Breakdown of the Spectator Concept in Low-Electron-Energy Resonant Decay Processes, *Phys. Rev. Lett.* **121**, 243002 (2018).
- [35] O. Jagutzki, V. Mergel, K. Ullmann-Pfleger, L. Spielberger, U. Spillmann, R. Dörner, and H. Schmidt-Böcking, A broad-application microchannel-plate detector system for advanced particle or photon detection tasks: large area imaging, precise multi-hit timing information and high detection rate, *Nucl. Instrum. Methods Phys. Res., Sect. A* **477**, 244 (2002).
- [36] O. Jagutzki, J. S. Lapington, L. B. C. Worth, U. Spillmann, V. Mergel, and H. Schmidt-Böcking, Position sensitive anodes for MCP read-out using induced charge measurement, *Nucl. Instrum. Methods Phys. Res., Sect. A* **477**, 256 (2002).
- [37] R. M. Wood, Q. Zheng, A. K. Edwards, and M. A. Mangan, Limitations of the axial recoil approximation in measurements of molecular dissociation, *Rev. Sci. Instrum.* **68**, 1382 (1997).
- [38] T. Weber, O. Jagutzki, M. Hattass, A. Staudte, A. Nauert, L. Schmidt, M. H. Prior, A. L. Landers, A. Bräuning-Demian, H. Bräuning, C. L. Cocke, T. Osipov, I. Ali, R. Díez Muiño, D. Rolles, F. J. García de Abajo, C. S. Fadley, M. A. Van Hove, A. Cassimi, and H. Schmidt-Böcking, K-shell photoionization of CO and N₂: Is there a link between the photoelectron angular distribution and the molecular decay dynamics? *J. Phys. B: At., Mol. Opt. Phys.* **34**, 3669 (2001).

- [39] E. B. Saloman and C. J. Sansonetti, Wavelengths, energy level classifications, and energy levels for the spectrum of neutral neon, *J. Phys. Chem. Ref. Data* **33**, 1113 (2004).
- [40] M. Mucke, M. Förstel, T. Lischke, T. Arion, A. M. Bradshaw, and U. Hergenbahn, Performance of a short magnetic bottle electron spectrometer, *Rev. Sci. Instrum.* **83**, 063106 (2012).
- [41] M. Förstel, T. Arion, and U. Hergenbahn, Measuring the efficiency of interatomic coulombic decay in Ne clusters, *J. Electron Spectrosc. Relat. Phenom.* **191**, 16 (2013).
- [42] M. Mucke, T. Arion, M. Förstel, T. Lischke, and U. Hergenbahn, Competition of inelastic electron scattering and Interatomic Coulombic Decay in Ne clusters, *J. Electron Spectrosc. Relat. Phenom.* **200**, 232 (2015).
- [43] U. Buck and R. Krohne, Cluster size determination from diffractive He atom scattering, *J. Chem. Phys.* **105**, 5408 (1996).
- [44] A. Hans, C. Ozga, Ph Schmidt, G. Hartmann, A. Nehls, Ph. Wenzel, C. Richter, C. Lant, X. Holzapfel, J. H. Viehmann, U. Hergenbahn, A. Ehresmann, and A. Knie, Setup for multi-coincidence experiments of photons in the extreme ultraviolet to visible spectral range and charged particles-The solid angle maximization approach, *Rev. Sci. Instrum.* **90**, 093104 (2019).
- [45] R. Santra, J. Zobeley, L. S. Cederbaum, and N. Moiseyev, Interatomic Coulombic Decay in van der Waals Clusters and Impact of Nuclear Motion, *Phys. Rev. Lett.* **85**, 4490 (2000).
- [46] R. Flesch, N. Kosugi, A. Knop-Gericke, and E. Rühl, 2s-excitation and photoionization of neon clusters, *Z. Phys. Chem.* **228**, 387 (2014).
- [47] U. Hergenbahn, A. Kolmakov, M. Riedler, A. R. B. de Castro, O. Löffken, and T. Möller, Observation of excitonic satellites in the photoelectron spectra of Ne and Ar clusters, *Chem. Phys. Lett.* **351**, 235 (2002).
- [48] L. Ben Ltaief, A. Hans, P. Schmidt, X. Holzapfel, F. Wiegandt, P. Reiss, C. Küstner-Wetekam, T. Jahnke, R. Dörner, A. Knie, and A. Ehresmann, VUV photon emission from Ne clusters of varying sizes following photon and photoelectron excitations, *J. Phys. B: At., Mol. Opt. Phys.* **51**, 065002 (2018).
- [49] T. A. Carlson and M. O. Krause, Experimental Evidence for Double Electron Emission in an Auger Process, *Phys. Rev. Lett.* **14**, 390 (1965).
- [50] J. Viehhaus, S. Cvejanović, B. Langer, T. Lischke, G. Prümper, D. Rolles, A. V. Golovin, A. N. Grum-Grzhimailo, N. M. Kabachnik, and U. Becker, Energy and Angular Distributions of Electrons Emitted by Direct Double Auger Decay, *Phys. Rev. Lett.* **92**, 083001 (2004).
- [51] F. Penent, J. Palaudoux, P. Lablanquie, L. Andric, R. Feifel, and J. H. D. Eland, Multielectron Spectroscopy: The Xenon 4d Hole Double Auger Decay, *Phys. Rev. Lett.* **95**, 083002 (2005).
- [52] A. H. Roos, J. H. D. Eland, J. Andersson, R. J. Squibb, D. Koulentianos, O. Talae, and R. Feifel, Abundance of molecular triple ionization by double Auger decay, *Sci. Rep.* **8**, 16405 (2018).
- [53] A. C. LaForge, M. Shcherbinin, F. Stienkemeier, R. Richter, R. Moshhammer, T. Pfeifer, and M. Mudrich, Highly efficient double ionization of mixed alkali dimers by intermolecular Coulombic decay, *Nat. Phys.* **15**, 247 (2019).
- [54] A. Eckey, A. B. Voitkiv, and C. Müller, Resonant single-photon double ionization driven by combined intra- and interatomic electron correlations, *J. Phys. B: At., Mol. Opt. Phys.* **53**, 055001 (2020).